Outcome of Temporal Lobe Epilepsy Surgery Predicted by Statistical Parametric PET Imaging

Ching-Yee Oliver Wong, Eric B. Geller, Eric Q. Chen, William J. MacIntyre, Harold H. Morris III, Shanker Raja, Gopal B. Saha, Hans O. Lüders, Sebastian A. Cook and Raymundo T. Go
Departments of Nuclear Medicine and Neurology, Cleveland Clinic Foundation, Cleveland, Ohio

PET is useful in the presurgical evaluation of temporal lobe epilepsy. The purpose of this retrospective study is to assess the clinical use of statistical parametric imaging in predicting surgical outcome. **Methods:** Interictal ^{18}FDG-PET scans in 17 patients with surgically-treated temporal lobe epilepsy (Group A = 13 seizure-free, group B = 4 not seizure-free at 6 mo) were transformed into statistical parametric imaging, with each pixel representing a z-score value by using the mean and s.d. of count distribution in each individual patient, for both visual and quantitative analysis. **Results:** Mean z-scores were significantly more negative in anterolateral (AL) and mesial (M) regions on the operated side than the nonoperated side in group A (AL: $p < 0.00005$, M: $p = 0.0097$), but not in group B (AL: $p = 0.46$, M: $p = 0.08$). Statistical parametric imaging correctly lateralized 16 out of 17 patients. Only the AL region, however, was significant in predicting surgical outcome ($F = 29.03$, $p < 0.00005$). Using a cut-off z-score value of -1.5, statistical parametric imaging correctly classified 92% of temporal lobes from group A and 88% of those from Group B. **Conclusion:** The preliminary results indicate that statistical parametric imaging provides both clinically useful information for lateralization in temporal lobe epilepsy and a reliable predictive indicator of clinical outcome following surgical treatment.

Key Words: PET; temporal lobe epilepsy surgery; statistical parametric imaging

J Nucl Med 1996; 37:1094–1100

PET has shown to be useful in the localization of seizure foci for epilepsy surgery (*1–10*). Regions of cerebral glucose hypometabolism, detected interictally, correlate well with epileptogenic zones. These zones are determined by scalp EEG and depth electrode studies. Pathologic lesions are demonstrated at surgery and PET may correctly localize the seizure focus in 60%–90% of patients with temporal lobe epilepsy (*1–10*).

Routine clinical interpretation of PET images for hypometabolism depends on visual assessment on a continuous gray scale or semiquantitative color scale. This technique, relying on arbitrary scaling to the maximal uptake, may show variable relative glucose metabolism among patients, and sometimes even within different studies of the same patient. Comparison of homologous regions has been achieved using some type of asymmetry indices (*2,8*), typically based on quantitative regional cerebral glucose metabolism or semiquantitative count ratios in the regions of interest (ROIs) on the abnormal side in comparison to the contralateral side. The asymmetry indices technique is based on the assumption of having a relatively normal contralateral side and, thus, is not applicable in patients with bilateral abnormalities. Relative quantification is commonly achieved by count ratios which rely on the assumption of normal reference regions such as the visual cortex or cerebellum. Additionally, absolute quantification of regional glucose metabolism is usually performed using prolonged dynamic acquisition and requires invasive arterial blood sampling (*1,2*).

We developed a method of quantitative statistical parametric imaging, which allows comparison of ROIs based on deviations from the individual subject's mean cerebral glucose metabolism. This method measures abnormalities based on the patient's normal physiologic level of glucose metabolism and allows a simple quantitative analysis of PET images. The purpose of this retrospective study is to examine the utility of statistical parametric imaging in routine clinical interpretation of PET images for temporal lobe epilepsy and determine its ability to predict clinical outcome by using the site of surgery and seizure-free condition after temporal lobe resection as the gold standard. A portion of the present investigation has been reported in abstract form (*11*).

MATERIALS AND METHODS

Patients

Interictal PET images from 17 patients (10 men, 7 women; aged 5–49 yr; mean age 26.3 ± 11.7 yr) with temporal lobe epilepsy who had surgical resection were analyzed. These patients were referred by the neurology and neurosurgery departments from a group of seizure patients over a 1-yr period who had PET imaging as a part of presurgical evaluation for temporal lobectomy and had undergone follow-up for at least 6 mo after surgery at our institution. No patients were excluded based on PET data. Other presurgical evaluations included video-EEG monitoring with scalp and sphenoidal electrodes, MRI, intracarotid amobarbital testing (Wada procedure) and neuropsychological testing. Five patients underwent bi-temporal depth electrode recordings because of poor scalp EEG localization. PET data, analyzed by visual inspection of gray scale (Fig. 1A) and color (Fig. 1B) images were used as part of the decision to perform surgery, but statistical parametric imaging was not available preoperatively in any patient (Table 1).

The patient population was divided into two groups for analysis. Group A included 13 patients (8 males, 5 females; aged 5–38 yr; mean age 24.2 ± 9.9 yr) with good surgical outcome (defined as seizure-free at 6-mo follow-up) and Group B consisted of four patients (2 men, 2 women; aged 11–49 yr; mean age 33.0 ± 16.2 yr) with poor surgical outcome (defined as not seizure-free at 6-mo follow-up). A follow-up period of 6-mo was chosen based on the results of Lüders et al. (*12*), in which this time frame seems to be an excellent predictor of subsequent outcome. No statistically significant differences in the ages of these two groups ($p = 0.37$) were evident. The clinical data are summarized in Table 1.

Scintigraphic Methods

All patients imaged received an average dose of 290 ± 64 MBq [^{18}F]FDG. Scalp EEG monitoring was used in each patient before tracer injection and during the uptake period of [^{18}F]FDG. No patient had a seizure during PET imaging. Image acquisition began about 45 min after tracer injection. The camera's axial field of view consisted of 21 contiguous slices with an axial thickness of 5.125 mm. The in-plane resolution was 5.8 mm and the axial resolution

Received May 5, 1995; revision accepted Aug. 17, 1995.
For correspondence or reprints contact: C. Oliver Wong, MBBS, PhD, Department of Nuclear Medicine, Gb3, Cleveland Clinic Foundation, Cleveland, OH 44195.

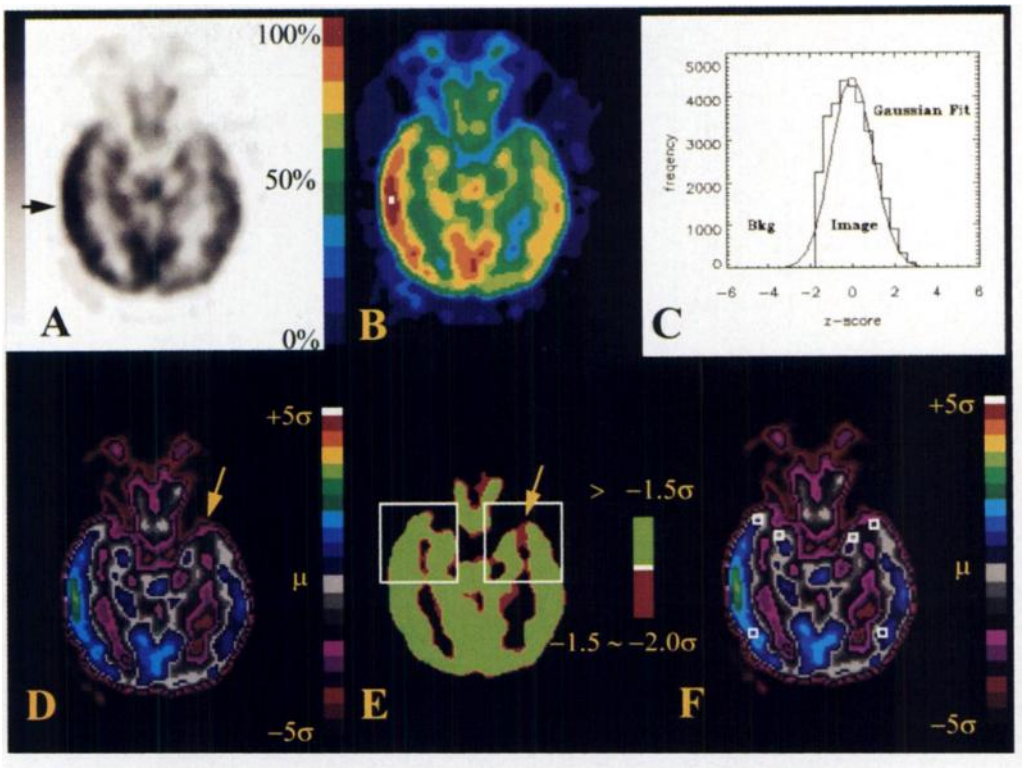

FIGURE 1. Transverse PET image (the left side of the image represents the right side of the patient) along the long-axis of the temporal lobe through the subthalamic region is shown with gray scale (A) and 10% color bar (B). These images show apparent reduction of activity in the cortex due to high activity at the mid-lateral neocortex of the right temporal lobe (black arrow) or (C) Gaussian distribution of pixels from gray matter. (D) Z-score statistical parametric imaging with each color interval representing 0.5 s.d. from the global mean (z-score value). (E) Abnormal areas defined as below −1.5 but above −2.0 s.d. (note the asymmetry enclosed by the square boxes). (F) The 4 × 4-pixel ROIs used in Student t-test and discriminant analysis.

was 11.9 mm FWHM. Attenuation correction was applied for each slice using separate elliptical ROIs defined interactively by the operator to trace the scalp. A uniform attenuation coefficient of 0.096 cm^{-1} was used. Reconstruction of a 256 × 256 image matrix with a pixel size of 1.7 mm was performed utilizing linear filtered backprojection with a Butterworth filter of order 10 and critical frequency of 0.04 cycle/mm. After filtering, the in-plane resolution became 15.5 mm FWHM. Each set of images were then transferred to a computer where they were further processed by re-orientation along the long-axis of the temporal lobe. Finally the transverse images were reformatted by summing into ten slices, each slice measuring 5 pixel thickness.

Statistical and Computer Analysis

The statistical parametric images were obtained by transforming counts from each pixel of the original PET images (Fig. 1A), $I_{(x,y)}$, into a z-score value (Fig. 1D), $Z_{(x,y)}$, using PV-WAVE ADVANTAGE (Visual Numerics, Boulder, CO), by the following formula:

$$Z_{(x,y)} = [I_{(x,y)} - \mu]/\sigma, \qquad \text{Eq. 1}$$

where μ and σ are the mean and s.d. of the pixel counts representing predominantly gray matter. In calculating μ and σ, pixels from the background, ventricles and most of the white matter were excluded by setting a 50% threshold of the

TABLE 1
Patient Data

Patient no.	Age (yr)	PET	EEG	MRI	Surgery	Pathology	Outcome	SPI
1	26	R	R	R HF atrophy	R	FNH	I	R
2	25	R	R	R HF atrophy	R	SPG, HFG	I	R
3	35	ND	R	Normal	R	SPG, FMF, FNH	I	L
4	28	R	R*	Normal	R	SPG	I	R
5	7	R	R	R HF atrophy	R	SPG	I	R
6	38	R	R	R HF atrophy	R	SPG, FNH	I	R
7	5	R	R	R TL mass	R	Astrocytoma	I	R
8	16	L	L	L TL mass	L	Dysplasia	I	L
9	30	L	L*	L HF atrophy	L	SPG	I	L
10	22	L	L	L HF atrophy	L	SPG, FNH	I	L
11	29	L	L	Normal	L	SPG, FMF, FNH	I	L
12	23	L	L	Normal	L	SPG, FMF	I	L
13	31	ND	L*	L HF atrophy	L	SPG, FNH, HFG	I	L
14	32	L	L*	Normal	L	SPG	IV	L
15	49	L	L	L HF atrophy	L	SPG, FMF, FNH	II	L
16	40	ND	L*	L HF atrophy	L	MTS, SPG, FNH	IV	L
17	11	L	L	L HF atrophy	L	MTS	IV	L

R = right; L = left; PET = the conventional reading of PET; Diagnostic (L, R) with more than 10% asymmetry, otherwise nondiagnostic (ND); * = depth electrode, otherwise just scalp EEG; HF = hippocampal formation; MTS = mesial temporal sclerosis; SPG = subpial gliosis; FMF = focal meningeal fibrosis; FNH = focal neuronal heteropia; HFG = HF gliosis; Outcome: I = seizure-free; II = less than or equal to 2 seizures per year; III = interpretation of more than two seizures per year with more than or equal to 90% improvement; IV = less than 90% improvement, no change or worse; SPI = the visual z-score transformation of PET and lateralization is defined as asymmetry in areas below −1.5 but above −2.0 s.d. of the mean.

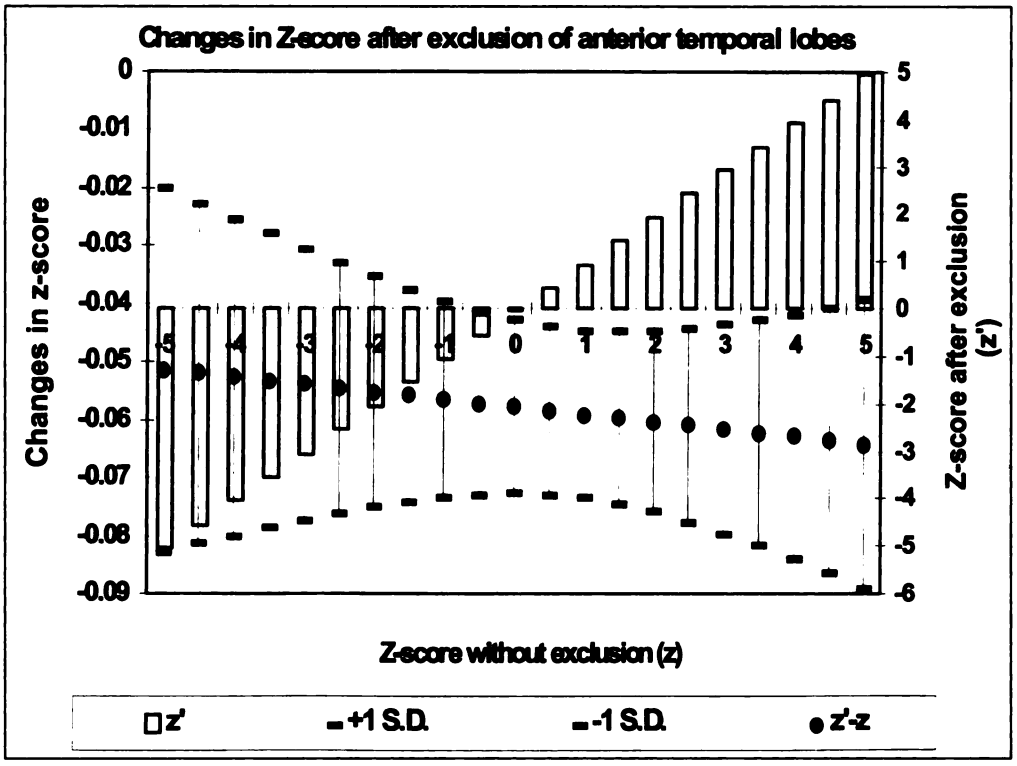

FIGURE 2. Changes in z-scores after exclusion of pixels from both anterior temporal lobes (where seizure foci are located) are plotted against the range of z-scores without exclusion of any pixels from any portion of brain tissue (x-axis). Due to the small amplitude of changes in z-scores (enlarged scale shown by y-axis on the left side, $z' - z$), one can hardly detect any changes in the z-scores calculated after exclusion (y-axis on the right side, z').

maximum pixel counts. Since over 20,000 pixels have been used, the pixel count distribution essentially follows a Gaussian function (Appendix and Fig. 1C). There were no significant, detectable changes in the z-score even when the pixels from abnormal temporal foci were excluded in the calculation of the global mean and s.d. (Appendix and Fig. 2).

Image Display and Analysis

The z-score statistical parametric imaging was displayed with 0.5 s.d. intervals, ranging from −5 to +5 s.d. (Fig. 1D) for visual interpretation. The color representation was chosen in such a way that it still provides a gradient from the lowest-to-highest pixel counts, which is a system that is often used by clinicians. In these parametric images, each color represents an additional interpretation of how far the glucose metabolic rate of a region deviates from the normal mean value which is represented at the center of the interval. The statistical parametric imaging was used directly for visual and quantitative analysis.

Visual analysis consisted of assessing the statistical parametric imaging for the location and size of the temporal lobe that deviated significantly from the mean. Lateralization was assisted by setting a threshold on statistical parametric imaging to show asymmetric differences in pixel areas below −1.5 but above −2.0 s.d. from the mean in the temporal lobes (Fig. 1E). The upper limit of −1.5 was justified by the results of discriminant analysis as described below

TABLE 2
Z-scores in Group A Patients with Good Clinical Outcome

	Epileptogenic side z-score			Contralateral normal side z-score		
Patient no.	AL*	M†	PL‡	AL*	M†	PL‡
1	−2.74	−2.26	0.35	−0.83	−1.39	−0.14
2	−2.68	−2.69	−0.10	−1.44	−1.77	0.21
3	−1.72	−1.45	−0.14	−0.86	−2.10	0.16
4	−1.00	−1.30	0.14	−0.28	−0.37	1.01
5	−3.41	−3.09	0.02	0.32	−0.90	0.15
6	−1.83	−2.04	0.25	−1.36	−1.37	0.43
7	−2.24	−2.63	−0.45	−0.67	−1.84	0.94
8	−2.49	−2.14	−0.05	−1.30	−1.96	−0.13
9	−1.86	−1.76	−0.30	−1.15	−0.95	−0.24
10	−2.20	−2.11	0.76	−0.82	−1.82	0.40
11	−1.98	−1.04	0.17	−0.50	−0.55	0.85
12	−2.02	−2.00	−0.04	−1.35	−0.62	0.94
13	−1.10	−1.74	0.05	−1.00	−2.05	−0.65
Mean ± s.d.	−2.10 ± 0.66	−2.02 ± 0.58	0.05 ± 0.30	−0.86 ± 0.50	−1.36 ± 0.62	0.30 ± 0.52

p-value: *AL region = <0.00005; †M region = 0.0097; ‡PL region = 0.1496.
AL = anterolateral; M = mesial; PL = posterolateral temporal regions.

and the lower limit of −2.0 was chosen so as to eliminate pixels from the ventricles and white matter.

Quantitative analysis was achieved by sampling numerical values of z-scores for Student t-test and discriminant analysis. The sampling was performed by placing three 4 × 4 pixel ROIs, one on each of the anterolateral (AL), mesial (M) and posterolateral (PL) temporal lobes (Fig. 1F) from a slice through the subthalamic region. The AL region was chosen at the anterior pole of the temporal lobe just lateral to the long axis of the temporal lobe. The M region was chosen to be placed at the anterior mesial temporal lobe. The PL is placed at posterior one-third of the temporal lobe. All these regions were consistently placed by a single operator with constant landmarks in relation to the temporal lobe orientated along its long-axis.

The average $z_{(x,y)}$ values of the anterolateral, mesial and posterolateral regions in the temporal lobe were calculated, while the data from both Groups A and B were analyzed by the Student t-test for lateralization. Stepwise discriminant analysis of $z_{(x,y)}$ values from all three regions of both temporal lobes, against an outcome variable of normal lobe or epileptogenic focus, was performed in Group A. The epileptogenic focus within the temporal lobe was defined as the seizure focus that was identified by scalp EEG or invasive depth electrode studies, successfully resected by surgery and proven by the good clinical outcome of seizure-free condition during the 6-mo follow-up after surgical resection. These criteria also gave rise to a mutually exclusive definition of a normal temporal lobe. The cut-off value of $z_{(x,y)}$ was obtained with the best discriminating power from the discriminant analysis and was used to analyze the Group B patients. Demographic group data were expressed as mean ± s.d. and were compared using the Student t-test. A p-value of less than 0.05 was considered statistically significant in all tests.

RESULTS

Visual Analysis of Statistical Parametric Imaging

The highest z-score is found to be at the visual cortex which is usually above positive one standard deviation. The majority of the brain tissue lies within positive and negative one standard deviation of the mean. This enables easy and direct visual identification of areas that deviate significantly from the mean. The maximum deviations are found to be at the anterior pole of the temporal lobe and no extratemporal abnormal deviations are observed in this population. The statistical parametric imaging reveals significant deviations from the mean at the mesial, extending towards the anterolateral regions of the temporal lobe with surgically-proven seizure focus in 16 of 17 patients as compared with 14 of 17 patients by conventional visual analysis of PET images as listed in Table 1. The only result with false localization by visual assessment of statistical parametric imaging comes from Patient 3 who has been considered nonlocalizing in the conventional interpretation of PET. In this patient, the mesial region is more hypometabolic on the left (nonoperated) side but the anterolateral region is more hypometabolic on the right (operated) side. Since the visual statistical parametric imaging analysis assumes that the total abnormal areas are defined by a threshold between −1.5 and −2.0 s.d., the left side is judged slightly more abnormal than the right side. This judgement, however, does not change the predictive value (see below) of the AL region for lateralization (Table 2) and outcome (Fig. 3A). As shown in Table 2, the z-score value at the AL region is more significantly negative ($p < 0.00005$) than that of the M region ($p = 0.0097$) in patients with good clinical outcome. Thus, the size of temporal lobe involvement probably shows only the extent of functional involvement, but the severity of disease might be better assessed by the magnitude of deviations at the more distant area (viz. the anterolateral region) from the mesial temporal lobe. The posterolateral region is rarely abnormal in this population of patients (see also Tables 2 and 3).

Quantitative Analysis of Statistical Parametric Imaging

The average $Z_{(x,y)}$ values from each ROI for Groups A and B are calculated and tabulated in Tables 2 and 3. There is a significant difference in z-scores in the AL and M regions in group A ($p < 0.00005$ and $p = 0.0097$, respectively) but not in Group B patients. The PL regions in either group A or B do not reach a statistically significant level. The finding (Table 2 and Fig. 3A) that the z-score values by statistical parametric imaging on the surgical epileptogenic side of Group A patients are significantly lower than those of the corresponding regions from the nonoperated normal side in the same group confirms our visual analysis of statistical parametric imaging for lateralization of seizure focus in temporal lobe epilepsy patients. The

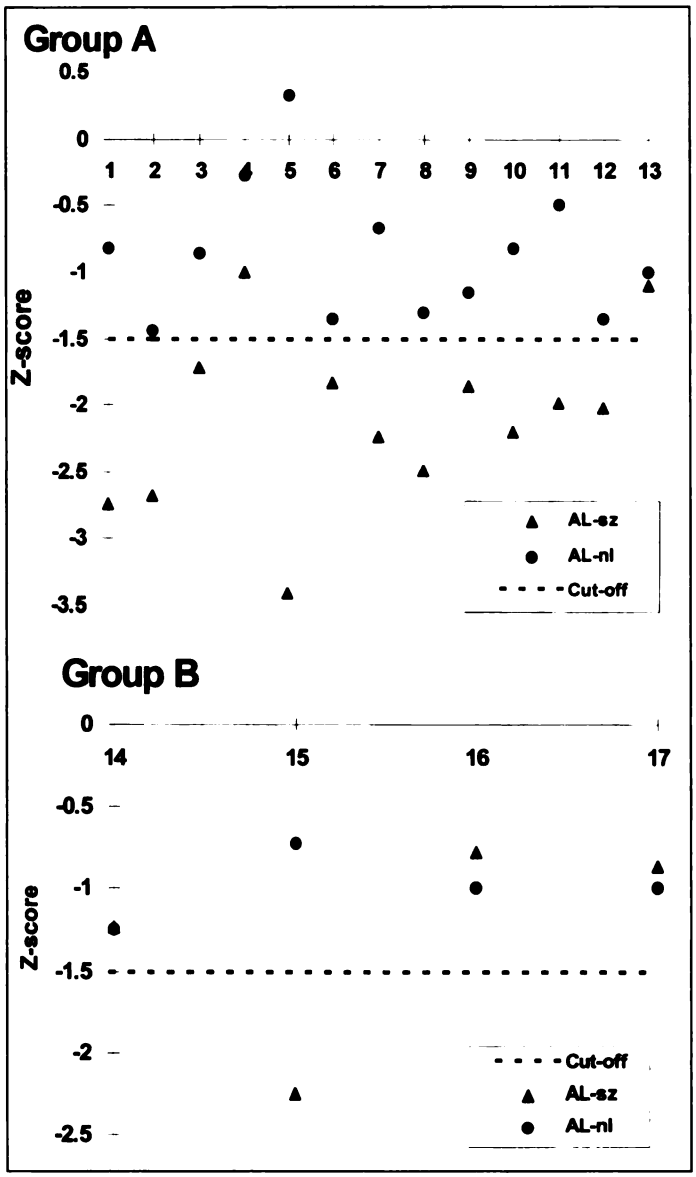

FIGURE 3. Scatter plots of the distribution of z-score values from the anterolateral region between the seizure side (AL-sz) and normal side (AL-nl) in Groups A and B. Note the clear separation of z-score values in Group A but the lack of discrimination of z-scores in Group B. The one exception is a patient who remained seizure-free after two typical seizures immediately following surgery.

TABLE 3
Z-scores in Group B Patients with Poor Clinical Outcome

Patient no.	Epileptogenic side z-score			Contralateral normal side z-score		
	AL*	M†	PL‡	AL*	M†	PL‡
14	−1.23	−2.01	−0.15	−1.24	−1.48	0.38
15	−2.25	−1.89	0.07	−0.72	−1.00	0.54
16	−0.78	−1.85	0.43	−1.00	−0.89	−0.43
17	−0.87	−3.19	−0.43	−1.00	−2.03	0.31
Mean	−1.28	−2.24	−0.02	−0.99	−1.35	0.20
s.d.	0.67	0.64	0.36	0.21	0.52	0.43

p-value: *AL regions = 0.46; †M regions = 0.08; ‡PL regions = 0.47.
AL = anterolateral; M = mesial; PL = posterolateral temporal regions.

conventional asymmetric index (AI), defined as the difference between right and left homologous regions divided by sum of these two regions shows a wide range of values. The AI varies from less than 1% to more than 20% in the mesial and anterolateral regions as shown in Table 4. On the contrary, the statistical parametric imaging reveals directly the asymmetry by showing the deviations from the global mean which is normalized to zero in statistical parametric imaging (Table 2 and Fig. 3A).

The stepwise discriminant analysis of $Z_{(x,y)}$ of group A patients indicates that only the AL region is significant in predicting seizure sites with clinical outcome of seizure-free condition after temporal lobectomy ($F = 29.03$, $p < 0.00005$). The M and PL regions do not contribute additionally in the prediction of seizure sites.

When the cut-off value of the z-score at −1.5 is chosen, the AL region correctly classifies 92% of the 26 temporal lobes from 13 patients in Group A with a sensitivity of 85% and specificity of 100% (Table 5). Conversely, only one of the eight AL regions in the temporal lobes from four patients in Group B has a z-score value less than −1.5 (Table 3 and Fig. 3B). Therefore, 88% of the eight temporal lobes are correctly classified using such a cut-off value. It is worth noting that the misclassified patient (No. 15 in Table 3) had only two typical seizures in the two months immediately after surgery but remained seizure-free over the subsequent 6-mo period. Because of our strict outcome criteria of seizure-free condition in the 6-mo time-point, this patient was placed in Group B but otherwise would have been placed in the good outcome group (Group A).

DISCUSSION

In this retrospective study, we used statistical parametric images to provide a quantitative imaging technique for localizing the temporal lobe with seizure foci in patients with temporal lobe epilepsy on routine clinical interpretation. The methodology takes into consideration how normal brain tissue in a given patient will behave and of variations, if any, among different regions. It tells whether a region is hyper- or hypometabolic based on the patient's internal physiologic standard. It is distinguished from other statistical parametric mappings, as discussed extensively in a recent review by Friston et al. (*13*), by its simplicity and being mathematically less demanding. Statistical parametric imaging carries more meaningful information than a simple count ratio by normalization to cerebella or visual cortices or as a percentage of maximal pixel counts which in the case of extremely high activity at the cerebellum or the visual cortex can cause erroneously low ratios at the

TABLE 4
Asymmetric Indices

Patient no.	Maximum seizure side (S)				Normal side (N)			Asymmetric index		
	Pixel counts	% Max			% Max			AI = (N − S)*100%/(N +S)		
		AL	M	PL	AL	M	PL	AL	M	PL
1	4903	39.2	44.0	70.2	58.4	52.7	65.3	19.6	9.0	−3.6
2	4931	39.6	39.5	64.9	51.7	48.5	67.9	13.3	10.2	2.3
3	4849	48.7	51.4	64.4	57.2	44.9	67.4	8.1	−6.7	2.3
4	4856	56.9	53.8	68.7	64.4	63.4	77.7	6.1	8.2	6.1
5	4836	32.0	35.3	67.7	70.8	58.1	69.1	37.8	24.4	1.0
6	4896	47.2	45.2	66.8	51.6	51.5	68.5	4.5	6.5	1.3
7	4802	43.5	39.5	62.0	59.8	47.6	76.4	15.7	9.4	10.4
8	4645	41.7	45.1	65.2	53.2	46.8	64.5	12.1	1.9	−0.6
9	4853	47.6	48.6	63.2	54.7	56.7	63.8	7.0	7.7	0.5
10	4831	44.3	45.2	74.0	58.2	48.1	70.4	13.5	3.1	−2.5
11	4714	47.3	46.7	67.7	61.3	60.8	74.1	12.9	13.2	4.6
12	4884	46.5	46.7	65.4	52.9	59.8	74.7	6.4	12.4	6.7
13	4908	54.3	48.8	64.1	55.1	46.2	58.1	0.8	−2.8	−4.9
14	4764	54.6	46.5	65.8	54.5	52.0	71.3	−0.1	5.6	4.0
15	4871	44.6	48.1	67.0	59.4	56.7	71.5	14.2	8.2	3.3
16	4868	59.0	48.6	70.8	56.9	57.9	62.4	−1.8	8.8	−6.3
17	4822	56.9	34.5	61.2	55.7	45.7	68.3	−1.1	14.0	5.5

%max = regional count ratios expressed as percentage of the maximum pixel counts.

TABLE 5
Classification of Patients in Group A

	PET (z-score < −1.5)	
Temporal lobes	Positive	Negative
Operated	11	2
Nonoperated	0	13

Sensitivity = 85%; specificity = 100%; accuracy = 92%.

cerebral cortices. The asymmetry observed in statistical parametric imaging is an absolute comparison to the internal standard, providing obvious information about lateralization. The asymmetric indices commonly used, however, are often calculated from the percentage of right and left count difference (*8,14*), based on the assumption of relative normality of the contralateral homologous regions which might not be true in epilepsy patients with bilateral seizure foci or other pathology in the contralateral region. Rather than relying on information from a single slice for asymmetry, statistical parametric imaging incorporates the normal metabolic status of the entire brain from a given individual in developing the concept of asymmetry in the image interpretation. Moreover, statistical parametric imaging not only provides the extent of abnormalities by the size of areas that deviate significantly from the mean but also the concept of severity by the magnitude of deviations from the mean. This might be the reason why statistical parametric imaging shows predictive ability of the clinical outcome.

Our outcome criteria were strict. We chose to define "good" outcome as being completely seizure-free after temporal lobectomy, because, presumably, the epileptogenic focus was correctly identified and resected in these patients. The patients included in this retrospective study all underwent temporal lobectomy. Although such patients are intensively investigated prior to temporal lobectomy, good postoperative seizure outcome represents the best "gold standard" in verifying a seizure focus. Further studies will be necessary to determine the ability of our statistical parametric imaging method for localization and prediction of outcome in patients with bilateral temporal or extratemporal foci.

We found that the most useful region for prediction of surgical outcome is the anterolateral region. This finding agrees with prior studies by Theodore et al. (*8*) and Sackellares (*14*), but disagrees with the study of Manno et al. (*15*) who found that the uncal region was the only region predictive of outcome. Other studies have found multiple areas of hypometabolism within and outside the temporal lobe, without any correlation of a particular area to outcome (*9,10,16*).

The cause of anterolateral hypometabolism remains controversial. Some authors have suggested that widespread hypometabolism may be due to physiological dysfunction in regions functionally associated with the mesial temporal lobe, rather than cell loss in these regions (*14,16*). Henry et al. (*17*) found no correlation between hypometabolism of any cortical region and the degree of hippocampal cell loss on pathology, suggesting that diaschisis due to cell loss alone cannot account for these findings. On the other hand, it might represent structural abnormality that is below the resolution of routine histopathological studies (*3*). Frost et al. (*18*) had demonstrated a significant elevation of μ-opiate receptor binding in the temporal neocortex ipsilateral to the seizure focus which coincides with the anterolateral glucose hypometabolism.

It is possible that the mixture of etiologies in these studies, including mesial temporal sclerosis and tumors, may have caused heterogeneous patterns on PET images. The results of the present study will need validation in a larger series with a more uniform etiology for seizure. Also, our findings of mesial regions being less significant than the anterolateral regions might be related to the limited resolution of our present PET system.

The statistical parametric imaging has several advantages over current qualitative and quantitative methods used for PET analysis. It is a simple quantitative method, avoiding the subjective bias in visual analysis and inter-observer variability (*5,8,15*). By using the individual's own mean cerebral glucose metabolism for comparison with each region, the statistical parametric imaging method avoids the possibility that patients with epilepsy may have global hypometabolism when compared to normal controls (*19*). Quantification using statistical parametric imaging avoids the need for invasive arterial blood

TABLE 6
Calculation of Means and Standard Deviations without (N) and with (N′) Exclusion of Anterior Temporal Lobes (Seizure Foci)

Patient no.	N	μ	σ	N′	μ'	σ'
1	31350	3268.33	490.84	28351	3291.53	492.75
2	28314	3247.46	483.26	26373	3273.76	482.47
3	31472	3190.74	483.10	27816	3229.80	486.58
4	29628	3265.43	500.51	26286	3303.87	500.04
5	26610	3264.20	504.05	25364	3285.49	501.62
6	27353	3154.77	461.52	24476	3172.90	465.60
7	24035	3202.69	497.10	22822	3221.15	496.53
8	34523	3052.02	446.91	31613	3077.23	449.18
9	33879	3214.33	486.25	31610	3245.54	483.82
10	26434	3207.72	485.17	23469	3236.78	490.19
11	30755	3114.40	447.72	27474	3138.39	449.03
12	28453	3210.48	465.82	26024	3233.73	467.67
13	28577	3122.82	416.87	26323	3152.10	415.52
14	30645	3209.90	495.61	27771	3251.15	493.19
15	29262	3231.15	469.60	26553	3259.59	469.39
16	32340	3241.36	473.35	29385	3275.06	472.63
17	28025	3150.61	465.61	26246	3168.09	467.35
Mean	29509	3196.97	474.90	26939	3224.48	475.50
s.d.	2744	60.25	22.80	2418	62.42	22.44

N = number of pixels; μ = mean; σ = standard deviation; N′ = remaining pixels.

drawing to estimate the local cerebral glucose metabolic rate (*1–5,14,16*). Yet, it provides nearly identical results as absolute measurement of glucose metabolic rate as reported in the literature (*14*). Statistical parametric imaging analysis can be rapidly performed using a workstation or even a personal computer, and displayed as a color scale image as well as providing numerical values of z-score for each pixel (Fig. 1D). It does not require the knowledge of normal profiles. It makes use of the assumption that the majority of brain regions in the interictal state have normal glucose metabolic rate in a particular individual. Regions with significant deviations for this normal mean value will be considered abnormal in that particular individual.

Our study cohort consists of seizure patients who have temporal lobectomy and a minimum of 6-mo follow-up in our institution. The extratemporal epileptic foci, which are not present in our present population, might also be detected by statistical parametric imaging analysis. Since the extratemporal focus has a different profile than temporal lobe epilepsy, it might, however, require a different cut-off value.

CONCLUSION

This retrospective study in a limited number of seizure subjects confirms prior studies showing that regions of hypometabolism in the temporal lobe have good agreement with other tests used in the presurgical evaluation. Our finding that anterolateral hypometabolism of less than -1.5 is predictive of good surgical outcome is important, because it is based on an objective, quantitative method of analysis that is easily and noninvasively performed. A prospective study including a large number of patients is in progress to further evaluate statistical parametric imaging analysis of PET images in seizure patients for the accuracy of localization and the ability of predicting surgical outcome.

APPENDIX

The mean (μ) and s.d. (σ) used for statistical parametric imaging is calculated from all the pixels whose counts are greater than 50% of the maximal count in a given individual. The number of pixels (N) used in the calculation is 29509 ± 2744. To prove that the inclusion of a small area of abnormality will not significantly affect the z-score value displayed in statistical parametric imaging to be detected visually, the whole anterior one-third of both temporal lobes are excluded before calculating the μ and σ. The new μ' and σ' are calculated from the remaining 26939 ± 2418 pixels (N') which is more than 8% less than the original number of pixels (N) (Table 6). The change in the z-score is calculated by the following formula:

$$z'_{(x,y)} - z_{(x,y)} = \frac{z_{(x,y)}(\sigma - \sigma') + (\mu - \mu')}{\sigma'}, \qquad \text{Eq. 2}$$

where $z'_{(x,y)}$ is the new z-score calculated with μ' and σ'.

By substituting the range of z-score values from -5.00 to $+5.00$ in the above equation, the changes in the z-score were negligible (Fig. 2). The mean change in z-score is -0.056 ± 0.004 which is far below the visual detectable range in statistical parametric imaging.

ACKNOWLEDGMENTS

We thank Dr. Youssef G. Comair from the Department of Neurosurgery and Dr. Thian Ng from the Division of Radiology for their advice.

REFERENCES

1. Abou-Khalil BW, Siegel GJ, Sackellares JC, Gilman S, Hichwa R, Marshall R. Positron emission tomography studies of cerebral glucose metabolism in chronic partial epilepsy. *Ann Neurol* 1987;22:480–486.
2. Engel J Jr, Kuhl DE, Phelps ME, Mazziotta JC. Interictal cerebral glucose metabolism in partial epilepsy and its relation to EEG changes. *Ann Neurol* 1982a;12:510–517.
3. Engel J Jr, Brown WJ, Kuhl DE, Phelps ME, Mazziotta JC, Crandall PH. Pathological findings underlying focal temporal hypometabolism in partial epilepsy. *Ann Neurol* 1982b;12:518–528.
4. Engel J Jr, Kuhl DE, Phelps ME, Crandall PH. Comparative localization of epileptic foci in partial epilepsy by PCT and EEG. *Ann Neurol* 1982c;12:529–537.
5. Engel J Jr, Henry TR, Risinger MW, Mazziotta JC, Sutherling WW, Levesque MF, Phelps ME. Presurgical evaluation for partial epilepsy: relative contributions of chronic depth-electrode recordings versus FDG-PET and scalp-sphenoidal ictal EEG. *Neurology* 1990;40:1670–1677.
6. Theodore WH, Katz D, Kufta C, Sato S, Patronas N, Smothers P, Bromfield E. Pathology of temporal lobe foci: correlation with CT, MRI and PET. *Neurology* 1990;40:797–803.
7. Fisher RS, Frost JJ. Epilepsy. *J Nucl Med* 1991;32:651–659.
8. Theodore WH, Sato S, Kufta C, Balish MB, Bromfield EB, Leiderman DB. Temporal lobectomy for uncontrolled seizures: the role of positron emission tomography. *Ann Neurol* 1992;32:789–794.
9. Swartz BE, Tomiyasu U, Delgado-Escueta AV, Mandelkern M, Khonsari A. Neuroimaging in temporal lobe epilepsy: test sensitivity and relationships to pathology and postoperative outcome. *Epilepsia* 1992;33:624–634.
10. Radtke RA, Hanson MW, Hoffman JM, et al. Temporal lobe hypometabolism on PET: predictor of seizure control after temporal lobectomy. *Neurology* 1993;43:1088–1092.
11. Wong CYO, Geller EB, Chen E, et al. Statistical parametric imaging: a new method of PET analysis highly predictive of outcome in temporal lobe epilepsy surgery [Abstract]. *Epilepsia* 1995;36(suppl 4):164.
12. Lüders H, Murphy D, Awad I, et al. Quantitative analysis of seizure frequency 1 week and 6, 12 and 24 mo after surgery of epilepsy. *Epilepsia* 1994;35:1174–1178.
13. Friston KJ. Statistical parametric mapping: ontology and current issues. *J Cereb Blood Flow Metab* 1995;15:361–370.
14. Sachellares JC, Siegel GJ, Aboukhalil BW, et al. Differences between lateral and mesial temporal metabolism interictally in epilepsy of mesial temporal origin. *Neurology* 1990;40:1240–1426.
15. Manno EM, Sperling MR, Ding X, et al. Predictors of outcome after anterior temporal lobectomy: positron emission tomography. *Neurology* 1994;44:2331–2336.
16. Henry TR, Mazziotta JC, Engel J Jr. Interictal metabolic anatomy of mesial temporal lobe epilepsy. *Arch Neurol* 1993;50:582–589.
17. Henry TR, Babb TL, Engel J Jr, Mazziotta JC, Phelps ME, Crandall PH. Hippocampal neuronal loss and regional hypometabolism in temporal lobe epilepsy. *Ann Neurol* 1994;36:925–927.
18. Frost JJ, Mayberg HS, Fisher RS, et al. Mu-opiate receptors measured by positron emission tomography are increased in temporal lobe epilepsy. *Ann Neurol* 1988;23:231–237.
19. Theodore WH, Fishbein D, Dubinsky R. Patterns of cerebral glucose metabolism in patients with partial seizures. *Neurology* 1988;38:1201–1206.